Chinese Chemical Letters 31 (2020) 2661–2667

Contents lists available at ScienceDirect

Chinese Chemical Letters

journal homepage: www.elsevier.com/locate/cclet

Communication

Construction of high-efficient visible photoelectrocatalytic system for carbamazepine degradation: Kinetics, degradation pathway and mechanism

Ruonan Guo[a], Li-Chao Nengzi[b], Ying Chen[a], Qingqing Song[a], Jianfeng Gou[a], Xiuwen Cheng[a,b,*]

[a] Key Laboratory of Western China's Environmental Systems (Ministry of Education) and Key Laboratory for Environmental Pollution Prediction and Control, Gansu Province, College of Earth and Environmental Sciences, Lanzhou University, Lanzhou 730000, China
[b] Academy of Economics and Environmental Sciences, Xichang University, Xichang 615000, China

ARTICLE INFO

Article history:
Received 11 February 2020
Received in revised form 8 March 2020
Accepted 25 March 2020
Available online 29 April 2020

Keywords:
Photoelectrocatalytic system
r-TNAs photoanode
AC/PTFE cathode
Carbamazepine degradation pathway

ABSTRACT

This study aimed to construct a photoelectrocatalytic (PEC) reaction system based on the self-made reduced TiO_2 NTAs (r-TNAs) photoanode and activated carbon/Polytetrafluoroethylene (AC/PTFE) cathode. It would be observed clearly that the degradation rate constant of carbamazepine (CBZ) over r-TNAs$_{(photoanode)}$-AC/PTFE$_{(cathode)}$ PEC system (0.04961 min^{-1}) was even higher than that of r-TNAs$_{(photoanode)}$-Pt$_{(cathode)}$ PEC system (0.04602 min^{-1}) with the assistance of visible light irradiation and +0.4 V external potential. Besides, in order to obtain optimized conditions, the influence of key parameters such as pH value, electric current density and electrolyte concentration were studied. Most importantly, photoelectrochemical (PECH) properties, reactive oxide species contribution, $^{\bullet}OH$ formation rate and CBZ degradation pathway were determined. The results illustrated that the excellent PEC degradation performance depended on the excellent photocatalytic property of r-TNAs photoanode and electron transfer property of photoelectrodes in r-TNAs$_{(photoanode)}$-AC/PTFE$_{(cathode)}$ PEC system. Therefore, the study demonstrated that the r-TNAs$_{(photoanode)}$-AC/PTFE$_{(cathode)}$ PEC system could be expected to replace metal-catalyzed cathodes depending on its excellent PEC performance activity and low cost as well as the reaction system possessed objective and practical application prospect.

Masses of pharmaceuticals are applied to prevention, diagnosis and treatment of diseases in humans and animals. However, it should be noted that most of pharmaceuticals are not completely degraded after application. As a result, the pharmaceutical metabolites and some unchanged forms of these compounds are excreted and subsequently enter the ecosystem. With the advances in analytical technology, more and more pharmaceutical have been found in various conventional wastewater treatment plants (WWTPs) and they were incompletely removed [1,2]. Carbamazepine (CBZ) is one of the most frequently detected pharmaceutical residues in water bodies thus far [3,4]. Mild intake would cause drowsiness, vomiting, ataxia, ambiguity, nystagmus, hallucinations and mental disorder, furthermore, severe intoxications could lead to hypotension, respiratory, seizures depression and coma [5]. Many studies have found residual CBZ was ubiquitous in various environmental substrates (soil, surface, and groundwater) [6]. However, CBZ and its metabolites is recalcitrant and have been almost no degradation during membrane bioreactor treatments (<20%) or conventional biological wastewater (<10%) in conventional WWTPs [7–9]. Therefore, efficient and cost-effective techniques are needed to stop the entry of CBZ into the aquatic environment.

Recently, advanced oxidation processes (AOPs) using ozone, Fenton and UV radiation have been required to remove CBZ from aquatic environments [10,11]. What's more, among various AOPs treatments, the one which was driven by natural light have become a topic of concern in the past few decades given the fact that it would reduce the need to high cost of lamps and system maintenance [12]. And various photocatalysts with visible-light-driven activity have been found to be efficient for CBZ degradation [13–15]. Whereas, most of the reported catalysts are in form of

* Corresponding author at: Key Laboratory of Western China's Environmental Systems (Ministry of Education) and Key Laboratory for Environmental Pollution Prediction and Control, Gansu Province, College of Earth and Environmental Sciences, Lanzhou University, Lanzhou 730000, China.
E-mail address: chengxw@lzu.edu.cn (X. Cheng).

https://doi.org/10.1016/j.cclet.2020.03.068
1001-8417/

nanoparticles which may be difficult to recycle leading to the risk of secondary pollution. Moreover, electrochemical advanced oxidation processes (EAOPs) have obtained more and more attention as a promising class of AOPs, which possessed considerable practical applicability because of high energy efficiency, amenability to automation, simple equipment, safety and *etc.* [16,17]. Recent years, the removal of CBA from EAOPs have been studied [18,19], but high electricity consumption of the EF process greatly limits its wide application [20].

In recent years, the combination of electrochemistry and photocatalysis (PC) formed the so-called photoelectrocatalytic (PEC) reaction system. Because the external potential would further promote the transport and separation of photoinduced e^- from anode to cathode, leading to an enhanced carrier separation efficiency and PEC performance with low energy input [21]. Besides, nanocatalysts can be fixed in the electrodes, which would effectively control secondary pollution caused by the loss of nanoparticles. Consequently, PEC treatment has drawn more and more attention. Particularly, PC and PEC with TiO_2 nano-tubes arrays (TNAs) have been demonstrated to be powerful wastewater treatment options [22,23]. However, it was notable that pristine TNAs exhibited a vital defect that TiO_2 possess wide band gap (~3.2 eV). Thus, the recombination rate of photogenerated carriers in TiO_2 is pretty high, resulting in a limited practical applicability. Based on previous studies, reduced TiO_2 NTAs (r-TNAs) photoelectrode, which was constructed *via* a facile microwave reduction treatment, could possess both enhanced visible light response and commendable photoinduced charge carriers separation efficiency [24]. As for cathode, activated carbon (AC)/Polytetrafluoroethylene (PTFE) composite was deserved consider. In recent years, it was expected to replace metal-catalyzed cathodes with ultra-high surface area materials such as graphite particles and AC. Compared with graphite, AC was cheaper and more highly porous. It has been used in hydrogen fuel cells with precious metal catalysts such as platinum and palladium [25]. Besides, PTFE has become a unique electrical properties, concluding low dielectric constant and low dielectric loss, which is very stable over a wide frequency range [26]. Notably, reported studies stated that AC/PTFE composite could be used as photoelectrodes to produce oxygen-containing active substances and lead to the purification of pollutants [27,28].

In this work, a PEC reaction system was designed and constructed by the self-made r-TNAs photoanode and AC/PTFE cathode. The PEC performance of this system was evaluated *via* CBZ removal reaction with the assistance of external potential and visible light irradiation. Besides, the excellent PEC performance mechanism, as well as, the visible light PEC degradation pathways of CBZ were proposed. To the best of our knowledge, this is the first report on decomposition of pollutants in the PEC system based on r-TNAs photoanode and AC/PTFE cathode.

The buying channels of chemical reagents used in this study and the details of photoanode and cathode preparation were illustrated in Texts S1–S3 of Supporting information.

PC degradation of CBZ (100 mL, 5 mg/L) was carried out in a self-made quartz photoreactor at room temperature (25 °C) with initial pH 4.22 of CBZ solution. It was notable that a 350 W arc xenon lamp having an optical density of 100 mW/cm^2 was used as an external light source, which was placed approximately 16 cm from the photoanode. As for degradation reaction, in detailed, photoelectrode and cathode were fixed vertically in the quartz photoreactor and then magnetically stirred (with a shaking rate of 80 rpm) for 30 min without external light source to establish an adsorption/desorption equilibrium. Subsequently, switched on the above-mentioned xenon lamp. At given time intervals, the concentrations of CBZ was determined *via* an UV–vis spectrophotometer (EVOLUTION300, Thermo Scientific). It should be illustrated that the 0.5 mol/L Na_2SO_4 solution acted as the supporting electrolyte. As for PEC performance, its reaction process was conducted *via* a similar procedure, in which Pt plate or AC/PTFE electrode was served as cathode. It should be noted that the AC/PTFE and Pt cathode were with an effective area of 2 cm^2 and 1 cm^2, respectively. In addition, +0.4 V external potential was provided and controlled by a dual output DC power supply (DH1715A-5).

Because the operating parameters would affect the reaction system degradation efficiency, the effects of key parameters such as pH value, electric current density and electrolyte concentration were optimized. The pH value of the reaction system was adjusted by 1 mol/L NaOH and 1 mol/L H_2SO_4. Besides, the electric current density was provided and controlled by a dual output DC power supply. Since the existing photogenerated holes (h^+) and photogenerated electrons (e^-) in reaction system can be converted into H_2O_2, hydroxyl radicals ($^{\bullet}OH$) and superoxide free radical ($O_2^{\bullet-}$) active species [29,30], it was important to determine the main active substances in the PEC system. Scavenging experiments using TBA, *p*-benzoquinone (BQ), Fe(II)-EDTA, ammonium oxalate monohydrate (AO) and $K_2Cr_2O_7$ were conducted, which were served as scavengers for $^{\bullet}OH$, $O_2^{\bullet-}$, H_2O_2, h^+ and e^- species, respectively [31]. Besides, to identify intermediate products, samples were analyzed using a HPLC-MS measurement through Waters HPLC (2010, U. S. A.) coupled with a triple-stage quadrupole mass spectrometer (Thermo Scientific TSQ Quantum Access MAX, U. S. A.) in positive-ion mode electrospray ionization (ESI^+). Separation was carried out using a C 18 HPLC capillary column (100 mm × 2.1 mm, i.d. 5 μm, Thermo, U. S. A.). A self-made mixed solution containing acetonitrile and DI water (v/v, 55%/45%) as eluent and the flow rate was set as 1 mL/min. Moreover, injection

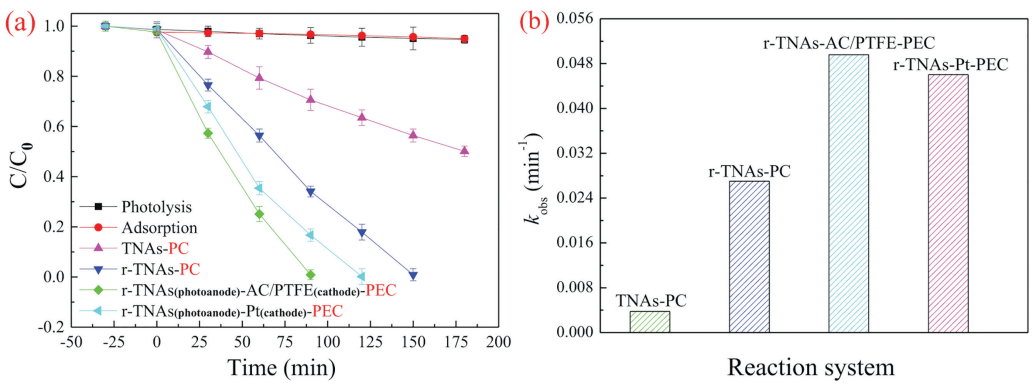

Fig. 1. PC and PEC degradation efficiency (a) and degradation rate constants (b) of CBZ in different single reaction system with definite experiment conditions.

volume of the sample, column temperature and excitation wavelength was maintained at 20 μL, 30 °C and 286 nm, respectively. Prior to detection, the mobile phase was filtered and sonicated to remove dissolved gases.

The photoelectrochemical (PECH) properties of the PEC system were detected using PQSTA 128 N electrochemical workstation in a traditional three-electrode configuration. The detailed detection methods were listed in Text S4 of Supporting information.

Fig. 1a exhibited the CBZ removal effect in various reaction systems, including the PC reaction system of r-TNAs and TNAs as well as the PEC reaction system of r-$TNAs_{(photoanode)}$-$AC/PTFE_{(cathode)}$. And the adsorption capability of r-$TNAs_{(photoanode)}$-$AC/PTFE_{(cathode)}$ reaction system and CBZ self-photodegradation performance were examined, with CBZ removal efficiency of 5.0% and 5.3%, respectively. With TNAs photoelectrode, the photocatalytic activity of reaction system would be significantly improved to 49.9% with the same experimental conditions. In particular, r-TNAs photoelectrode exhibited a more excellent PC performance compared with TNAs. Since bare TiO_2 is a wide band gap semiconductor, its excess amount would prevent visible-light absorption leading to a decreased photoactivity for pollutants removal. As for r-TNAs photoelectrode, a proper amount of TiO_2 has been reduced to be Ti^{3+} *via* a facile microwave reduction treatment. Therefore, the composite photoelectrode could be more favorable for efficient visible-light application and photoinduced charge carriers' separation. After inducing +0.4 V application voltage, the PEC reaction system of r-$TNAs_{(photoanode)}$-$AC/PTFE_{(cathode)}$ would exhibit the superior removal activities with CBZ removal efficiency of 99.1% within 90 min. Meanwhile, the CBZ degradation efficiency of r-$TNAs_{(photoanode)}$-$Pt_{(cathode)}$ PEC reaction system was determined as 99.1% within 120 min, proving the superior PEC performance of r-$TNAs_{(photoanode)}$-$AC/PTFE_{(cathode)}$. The fact would be further supported by the fitted kinetics constants of CBZ degradation process under xenon lamp irradiation with the assistance of +0.4 V application voltage. Fig. 1b displayed the degradation rate constant (k_{obs}) of the above-mentioned reaction systems which followed *pseudo* first-order kinetic equation. It would be clearly that the degradation rate constant of CBZ over r-$TNAs_{(photoanode)}$-$AC/PTFE_{(cathode)}$ PEC system was even higher than that of r-$TNAs_{(photoanode)}$-$Pt_{(cathode)}$ PEC system under the same irradiation conditions. Moreover, compared with another AOPs treatment methods (Table S1 in Supporting information), r-$TNAs_{(photoanode)}$-$AC/PTFE_{(cathode)}$ PEC system exhibited a more excellent CBZ removal performance. Therefore, it was reasonable to illustrate that the r-$TNAs_{(photoanode)}$-$AC/PTFE_{(cathode)}$ PEC system could be expected to replace metal-catalyzed cathodes depending on its excellent PEC performance activity and low cost.

Generally, various pH values would play different roles in photocatalytic process, because pH can influence the electron transfer process, surface electrical properties of the photoelectrode, ionization state of the organic compound and the formation of the reactive oxidizing species. Hence, the effect of pH value on the r-$TNAs_{(photoanode)}$-$AC/PTFE_{(cathode)}$ PEC reaction system was studied and presented in Fig. 2a. It was clearly that the degradation efficiency of CBZ was decreased from 87.7% to 82.2% as pH value increasing from 7 to 11. The result was attributed to that the surface charge of the catalyst would be different with the increase of pH value. Besides, as the pH decreased further, the PEC reaction system was turned to acidity, so that the significant increase of CBZ removal efficiency was achieved. When the pH value was changed from 5 to 4.22, the degradation efficiency of CBZ enhanced from 92.5% to 99.1%. Similarly, the regularities of degradation rate constants were consistent with that of degradation rate constant. Therefore, both of the highest PEC degradation efficiency and reaction rate occurred at pH value of 4.22. The difference of degradation efficiency trend with various pH value might be ascribed to the following description: Firstly, because the photocatalytic process mainly occurred on the surface of photoelectrodes rather than in the solution. Consequently, the adsorption capability of the r-$TNAs_{(photoanode)}$-$AC/PTFE_{(cathode)}$ surface played an important role in this PEC oxidation reaction [32]. It was reported that the difference between the pH of the solution and the pH_{PZC} of the catalyst was dominant to the catalyst surface charge property, which would affect the adsorption property of the electrode surface significantly [33]. According to previous study, the isoelectric point was 3.6 with the presence of Ti^{3+} introduced at the surface of TiO_2 [34]. Hence, the pH value was more closed to 3.6, better CBZ degradation performance in r-$TNAs_{(photoanode)}$-AC/

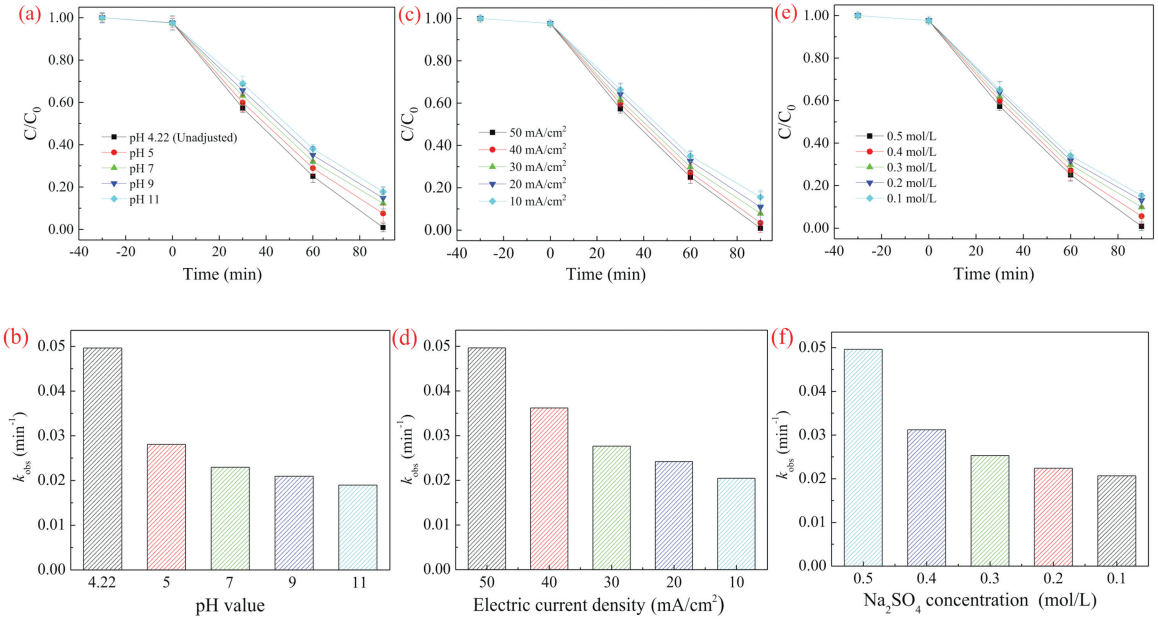

Fig. 2. The effects of pH value: (a) CBZ degradation efficiency and (b) degradation rate constants; The effects of electric current density: (c) CBZ degradation efficiency and (d) degradation rate constants; The effects of Na_2SO_4 concentration: (e) CBZ degradation efficiency and (f) degradation rate constants.

PTFE$_{(cathode)}$ PEC reaction system would be achieved. Hence, in the study, the further study would be performed with unadjusted pH in CBZ solution.

The electric current density is an influential parameter during the PEC reaction system for organic pollutants degradation process [35]. Fig. 2c presented the effect of current density on CBZ degradation using 0.5 mol/L Na_2SO_4 as supporting electrolytes. With the current density changing from 50 mA/cm^2 to 10 mA/cm^2, CBZ degradation efficiency decreased significantly. Moreover, it was observed in Fig. 2d that the degradation reaction followed *pseudo* first-order kinetic equation. The degradation rate constant of CBZ over r-TNAs$_{(photoanode)}$-AC/PTFE$_{(cathode)}$ PEC system was depended on current density as well. The degradation rate constant of CBZ over r-TNAs$_{(photoanode)}$-AC/PTFE$_{(cathode)}$ PEC system with 50 mA/cm^2 electric current density was pretty higher than another systems. The popularity of PEC reaction system was based on that the organic could be oxidized by direct electron transfer to the anode and/or oxidized by $^{\bullet}$OH, formed from water discharge on the anode surface under a high current [36]. However, it has been reported that with a much too high electric current density, there might be arisen masses of gas, resulting in a decrease in the diffusion layer. This phenomenon would lower the mass transfer coefficient, leading to an inefficient organics oxidation [37]. Taking the application cost, when the electric current density was 50 mA/cm^2, majority of CBZ (98.1%) would be destroyed. Hence, 50 mA/cm^2 was suitable for CBZ removal over r-TNAs$_{(photoanode)}$-AC/PTFE$_{(cathode)}$ PEC system, rather than a higher electric current density.

The concentration of supporting electrolyte plays important role in electron conduction process, which is related to the electrical consumption in PEC reaction system. Therefore, it was essential to detect the influence of electrolyte concentration on the CBZ removal performance in r-TNAs$_{(photoanode)}$-AC/PTFE$_{(cathode)}$ PEC system. As shown in Fig. 2e, with the Na_2SO_4 concentration turned from 0.1 mol/L to 0.5 mol/L, CBZ degradation efficiency exhibited a significantly increase. In particular, the degradation rate constant of CBZ over r-TNAs$_{(photoanode)}$-AC/PTFE$_{(cathode)}$ PEC system possessed a greater degree of transformation. The as-obtained PEC reaction system with 0.5 mol/L Na_2SO_4 exhibited the largest degradation rate constant value of 0.04961 min^{-1} (Fig. 2f). The superior removal efficiency and degradation rate constant of CBZ were achieved by r-TNAs$_{(photoanode)}$-AC/PTFE$_{(cathode)}$ PEC system with 0.5 mol/L Na_2SO_4. The formation of $^{\bullet}$OH on the surface of r-TNAs$_{(photoanode)}$ and AC/PTFE$_{(cathode)}$ can be explained by Eq. 1 [38]:

$$M(H_2O) \rightarrow M(^{\bullet}OH) + H^+ + e^- \quad (1)$$

When the Na_2SO_4 concentration changing from 0.4 mol/L to 0.5 mol/L in r-TNAs$_{(photoanode)}$-AC/PTFE$_{(cathode)}$ PEC system, the removal efficiency and degradation rate constant enhanced significantly, which could be explained by the following Eq. 2 [39]:

$$SO_4^{2-} \rightarrow SO_4^{\cdot -} + e^- \quad (2)$$

Both of $^{\bullet}$OH and sulfate radical ($SO_4^{\bullet -}$) radicals possessed high redox potential, which made them have excellent oxidative degradation properties for pollutants. Hence, the concentration of supporting electrolyte was optimized as 0.5 mol/L for CBZ removal over r-TNAs$_{(photoanode)}$-AC/PTFE$_{(cathode)}$ PEC reaction system.

The scavenging experiments were performed to investigate the contribution of reactive oxide species during CBZ degradation process in r-TNAs$_{(photoanode)}$-AC/PTFE$_{(cathode)}$ PEC reaction system. In detail, using TBA, BQ, Fe(II)-EDTA, AO and $K_2Cr_2O_7$ served as scavengers for $^{\bullet}$OH, $O_2^{\bullet -}$, H_2O_2, h^+ and e^- species, respectively. As displayed in Fig. 3a, PEC degradation system with TBA induction

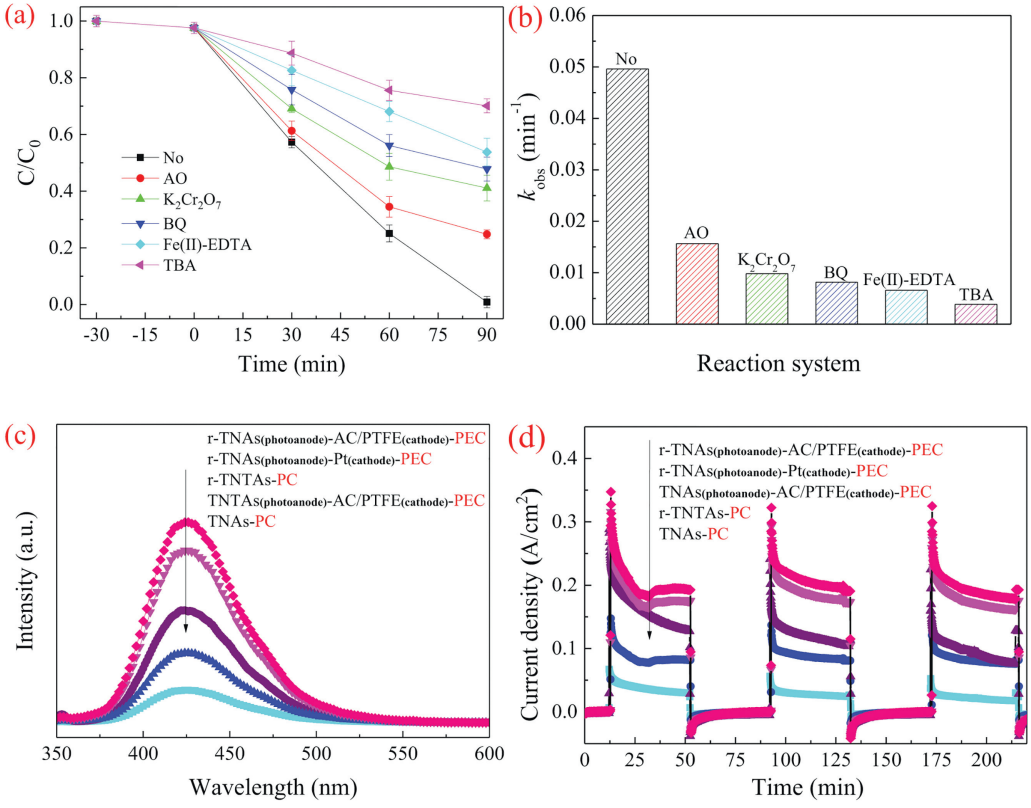

Fig. 3. PC and PEC degradation rates (a) and degradation rate constants (b) of CBZ in different scavenging reaction systems with definite experiment conditions; (c) Fluorescence spectra of as-constructed photoelectrodes; (d) Photocurrent density (*vs.* SCE) in PC and PEC systems.

would obtain the lowest CBZ removal efficiency, followed by Fe(II)-EDTA, BQ, $K_2Cr_2O_7$ and AO. Thus, it was preliminarily proved that ·OH was the most active species. What was more, the kinetics of the degradation process, which followed *pseudo* first-order kinetics equation, would further determine the contribution of the above-mentioned reactive species. As shown in Fig. 3b, the degradation rate constant of r-TNAs$_{(photoanode)}$-AC/PTFE$_{(cathode)}$ PEC reaction system was pretty higher than that of scavenging experiments. Therefore, it could be concluded that all of above-mentioned reactive species played oxide roles in CBZ degradation process, particularly, ·OH was the most superior active species.

Hydroxyl radicals (·OH) was determined as the dominant reactive species during CBZ degradation process in r-TNAs$_{(photoanode)}$-AC/PTFE$_{(cathode)}$ PEC system. Therefore, the production rate of ·OH at the sample/water interface was investigated *via* fluorescence spectra under the 350 W arc xenon lamp irradiation for as-prepared reaction systems. As shown in Fig. 3c, in PC reaction systems, the fluorescence spectra of bare TNAs exhibited a much lower production rate of ·OH compared with r-TNAs, illustrating the microwave reduction strategy was an efficient TNAs modification method. The increase of ·OH production rate indicated that the reaction capacity was improved, and the photocatalytic degradation efficiency of r-TNAs was improved, which was consistent with the photocatalytic degradation experimental results. As for PEC processes, r-TNAs$_{(photoanode)}$-AC/PTFE$_{(cathode)}$ PEC reaction system exhibited the strongest fluorescence intensity, indicating the

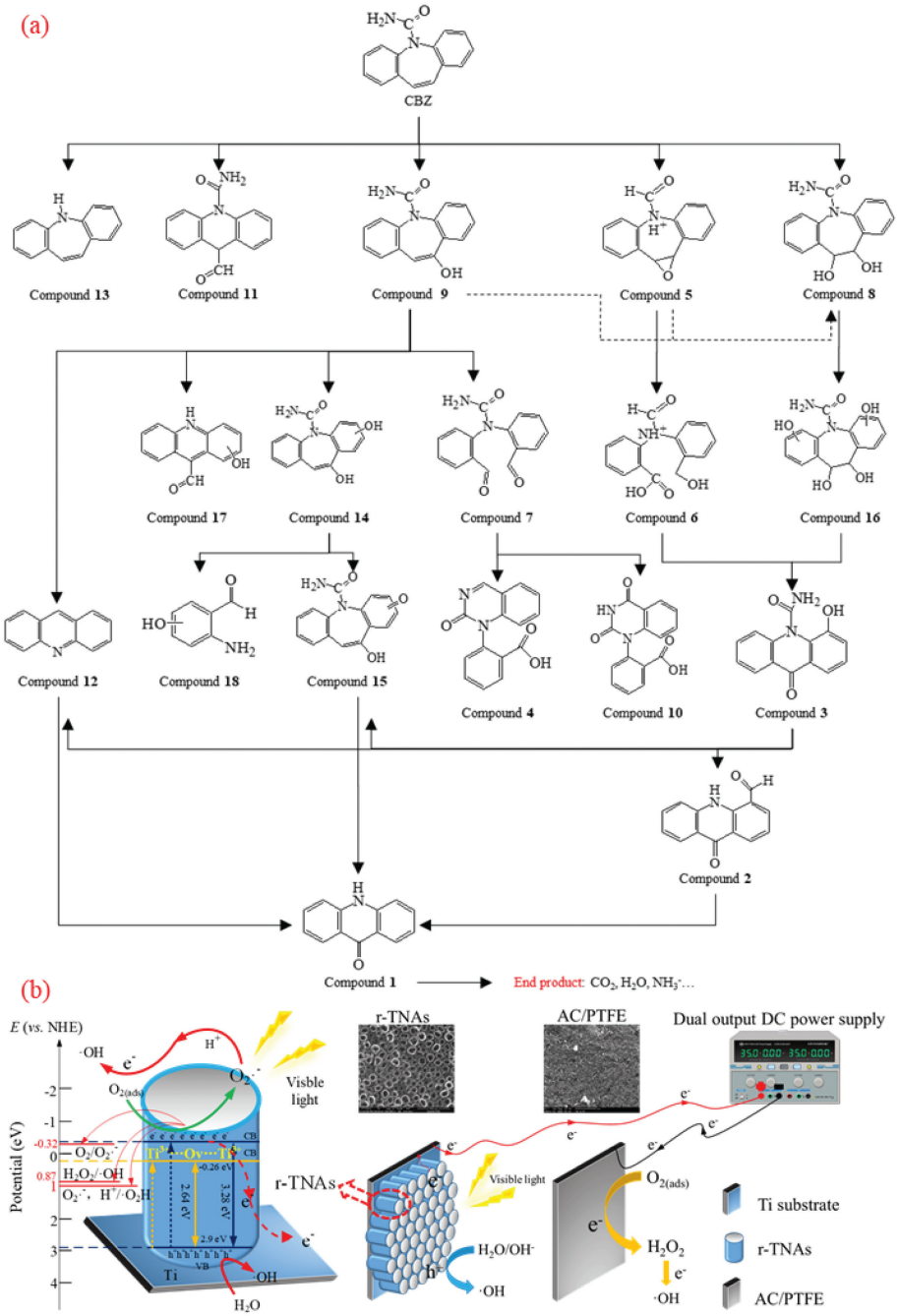

Fig. 4. (a) Proposed structures for the degradation products of CBZ identified using LC–MS. (b) The enhanced PC mechanism of r-TNAs photoanode, and PEC mechanism in PEC systems based on r-TNAs photoanode and AC/PTFE cathode.

highest production rate of $^{\bullet}OH$. Consequently, it was proved that the external potential significantly improved the fluorescence spectra intensity, indicating an increase in the production rate of $^{\bullet}OH$. The result would be explained by that the applied potential promoted the transfer and separation capability of e^- from the anode to the cathode, improving the photoinduced charge carriers' separation efficiency and the PEC reaction performance. Moreover, it can be clearly observed that the intensity of 2-hydroxyterephthalia acid (TAOH), which derived from the reaction between TPA and $^{\bullet}OH$ in r-TNAs$_{(photoanode)}$-AC/PTFE$_{(cathode)}$ PEC reaction system, was higher than that of the r-TNAs$_{(photoanode)}$-Pt$_{(cathode)}$ system. The result might be resulted from the contribution of r-TNAs$_{(photoanode)}$ and AC/PTFE$_{(cathode)}$, which both could catalyze adsorbed oxygen species to produce H_2O_2 and $^{\bullet}OH$, respectively. Therefore, the highest photocatalytic efficiency of r-TNAs$_{(photoanode)}$-AC/PTFE$_{(cathode)}$ PEC reaction system depended on the crucial actions of large amount of $^{\bullet}OH$.

PECH is an effective method to further explore the photocatalytic mechanism. Hence, the transient photocurrent response test was carried out to detect the separation and migration property of photogenerated carriers on surface of photoanodes. Fig. 3d exhibited the transient photocurrent response of r-TNAs and TNAs photoanodes under intermittent illumination in PC and PEC reaction systems. It was clearly that the r-TNAs$_{(photoanode)}$-AC/PTFE$_{(cathode)}$-PEC system was with the superior photoresponse capability and photocurrent intensity, indicating the most efficient separation of the photogenerated electron-hole pairs. Moreover, the data of transient photocurrent response could serve as a proof to prove the r-TNAs$_{(photoanode)}$-AC/PTFE$_{(cathode)}$-PEC system possessed a considerable stability. It was attributed to that the existence of Ti^{3+} would not only enhance photocatalytic performance but also be conductive to the stability of r-TNAs. Therefore, the highest degradation efficiency over r-TNAs$_{(photoanode)}$-AC/PTFE$_{(cathode)}$-PEC reaction system was the synthetic actions of the efficient separation of the photogenerated electron-hole pairs and enhanced transient photocurrent response.

During the CBZ degradation process in r-TNAs$_{(photoanode)}$-AC/PTFE$_{(cathode)}$ system, masses of intermediate products would be produced by the non-selective oxidation process of various reactive oxide species. More importantly, some by-products may incur agglomerate to biotoxicity. In this study, the intermediate products of CBZ was detected by HPLC coupled with MS measurements and the spectra was exhibited in Fig. S1 (Supporting information). Besides, based on the fragmentation patterns and molecular ionspeaksm, the calculated empirical formula of intermediates were proposed and summarized in Table S2 (Supporting information). Meanwhile, the degradation pathway of CBZ in r-TNAs$_{(photoanode)}$-AC/PTFE$_{(cathode)}$ PEC reaction system was depicted in Fig. 4a. Key points of the intermediate products identification were exhibited in Text S5 of Supporting information.

According to the previous studies, the CBZ degradation pathways such as TiO_2 photocatalysis [40], Fe(II)/persulfate [41] and solar photo-Fenton/persulfate [42] were also investigated. CBZ degradation intermediate products such as 10,11-dihydro-carbamazepine-10,11-epoxide (*m/z* 269, compound **8**), *N*-aminocarbonyl acridine-9-formaldehyde (*m/z* 253, compound **11**), hydroxy-(9*H*, 10*H*)-acridine-9-aldehyde (*m/z* 224, compound **17**) and acridine (*m/z* 180, compound **12**) were corresponding to our results. However, some of the detected products exhibited different structures due to different removal treatment. It should be noted that compared with those above-mentioned studies, there were more detailed intermediate products in the r-TNAs $_{(photoanode)}$-AC/PTFE $_{(cathode)}$-PEC system, a more comprehensive degradation pathway of CBZ were proposed.

Based on the above-mentioned experimental results and analysis, the mechanism of an enhanced PEC performance in r-TNAs$_{(photoanode)}$-AC/PTFE$_{(cathode)}$-PEC system would be deduced. Above all, it was essential to illustrate the mechanism of enhanced PC properties of r-TNAs photoelectrode. As exhibited in Fig. 4b, the impurity level which was near the conduction band (CB) of r-TNAs was induced due to the formation of Ti^{3+} and oxygen vacancies after microwave reduction treatment. The e^- in valence band (VB) of r-TNAs would be excited to the self-doping level rapidly and further near to r-TNAs VB with visible light irradiation. In addition, e^- can migrate onto the surface of r-TNAs and further react with adsorbed O_2 forming $O_2^{\bullet-}$, which would be further involved in CBZ removal process. At the same time, h^+ would oxidize CBZ directly or react with OH^- and H_2O forming $^{\bullet}OH$, which played the dominant role in CBZ degradation reaction. As such, compared with bare TNAs, r-TNAs photoelectrode possessed an excellent PC performance. Hence, we coupled r-TNAs$_{(photoanode)}$ with AC/PTFE$_{(cathode)}$ to build a PEC system for CBZ degradation with visible light irradiation and external potential.

Moreover, based on the experimental result, both of the r-TNAs photoanode and AC/PTFE cathode applied in the system possessed its proper characteristics, which were beneficial to enhance the PEC properties. As shown in Fig. 4b, when the light was switched on, photoinduced e^- in VB of r-TNAs photoanode would be excited and immigrant into the CB of r-TNAs, leaving excessive h^+ in the VB of r-TNAs (Eq. 3). The residual h^+ in the VB of r-TNAs also reacted with OH^- and H_2O in the solution to generate amount of $^{\bullet}OH$ (Eq. 4).

$$r-TNAs_{(photoanode)} + h\nu \rightarrow e^-_{(photoanode)} + h^+_{(photoanode)} \quad (3)$$

$$O_2 + 2H^+ + 2e^-_{(cathode)} \rightarrow H_2O_2 \quad (4)$$

Subsequently, the redundant e^- immediately transferred to the back contact electrode (Ti substrate). At the same time, with the existent external potential, bulk of e^- gradually migrate to the cathode (Eq. 5). So that the photogenerated e^- and h^+ pairs can be effectively separated. As a result, photogenerated e^- in AC/PTFE cathode and the remained h^+ in r-TNAs photoanode can react with the absorbed oxygen-containing species and H_2O, respectively, generating various active species (such as $^{\bullet}OH$) (Eqs. 6–8). Besides, in an acidic or neutral environment, the AC/PTFE cathode can catalyze the absorption O_2 to produce H_2O_2 and $^{\bullet}OH$ species (Eq. 9). These active species were responsible for the mineralization of CBZ, leading to the excellent PEC activity of r-TNAs$_{(photoanode)}$ with AC/PTFE$_{(cathode)}$ system (Eq. 10).

$$e^-_{(photoanode)} \rightarrow e^-_{(cathode)} \quad (5)$$

$$h^+_{(photoanode)} + O_2 \rightarrow O_2^{\bullet-} \quad (6)$$

$$O_2^{\bullet-} + 2H_2O \rightarrow H_2O_2 + 2^{\bullet}OH \quad (7)$$

$$e^-_{(cathode)} + OH^-/H_2O \rightarrow {}^{\bullet}OH \quad (8)$$

$$AC/PTFE\ cathode + absorded\ O_2/OH^-/H_2O \rightarrow H_2O_2 + {}^{\bullet}OH \quad (9)$$

$$h^+_{(photoanode)}/{}^{\bullet}OH/O_2^{\bullet-} + CBZ \rightarrow degraded\ products \quad (10)$$

In conclusion, a PEC reaction system was constructed successfully based on the self-made AC/PTFE cathode and r-TNAs photoanode. Favorable PEC performance in r-TNAs$_{(photoanode)}$-AC/PTFE$_{(cathode)}$ reaction system for CBZ removal (99.1%) was detected

with the assistance of visible light irradiation and +0.4 V external potential. Furthermore, it would be observed clearly that the degradation rate constant of CBZ over r-TNAs$_{(photoanode)}$-AC/PTFE$_{(cathode)}$ PEC system (0.04961 min^{-1}) was even higher than that of r-TNAs$_{(photoanode)}$-Pt$_{(cathode)}$ PEC system (0.04602 min^{-1}) under the same irradiation conditions. Besides, effects of reaction parameters were investigated in detail, demonstrating the optimal experimental conditions was with 40 mA/cm^2 electric current density and 0.5 mol/L electrolyte concentration. More importantly, in order to explain the enhanced PEC mechanism, different reactive oxide species involvement, $^{\bullet}$OH formation rate and photocurrent response performance of r-TNAs$_{(photoanode)}$-AC/PTFE$_{(cathode)}$ reaction system were detected. And the visible light PEC degradation pathways of CBZ were proposed, including hydroxylation and oxidation processes. Hence, the dominant oxide role of $^{\bullet}$OH in CBZ degradation process was determined. The radical with strong oxidation was generated based on the enhanced transient photocurrent response of r-TNAs and efficient separation of photogenerated carriers in PEC reaction system. Therefore, the study provided a PEC system which was expected to replace metal-catalyzed cathodes depend on its excellent PEC performance activity and low cost, so that it could be look forward to applying to remove residual antibiotics in wastewater for environment remediation.

Declaration of competing interest

We have no conflicts of interest to declare.

Acknowledgments

This work was kindly funded by National Natural Science Foundation of China (Nos. 51508254, 51978319), Fundamental Research Funds for the Central Universities (No. lzujbky-2017-it98), National College Student Innovation and Entrepreneurship Training Program of Lanzhou University and Key Laboratory of Comprehensive and Highly Efficient Utilization of Salt Lake Resources, Qinghai Institute of Salt Lake, Chinese Academy of Sciences.

Appendix A. Supplementary data

Supplementary material related to this article can be found, in the online version, at doi:https://doi.org/10.1016/j.cclet.2020.03.068.

References

[1] B. Yang, G.G. Ying, J.L. Zhao, et al., Water Res. 46 (2012) 2194–2204.
[2] A. Jelic, C. Cruz-Morató, E. Marco-Urrea, et al., Water Res. 46 (2012) 955–964.
[3] Y. Zhang, S.-U. Geißen, C. Gal, Chemosphere 73 (2008) 1151–1161.
[4] M. Clara, B. Strenn, O. Gans, et al., Water Res. 39 (2005) 4797–4807.
[5] D.P. Mohapatra, S.K. Brar, R.D. Tyagi, et al., Sci. Total Environ. 470–471 (2014) 58–75.
[6] R. Zhou, J. Zhao, N. Shen, et al., Chemosphere 197 (2018) 670–679.
[7] M. Clara, B. Strenn, N. Kreuzinger, Water Res. 38 (2004) 947–954.
[8] J. Deng, Y. Shao, N. Gao, et al., Chem. Eng. J. 228 (2013) 765–771.
[9] P. Braeutigam, M. Franke, R.J. Schneider, et al., Water Res. 46 (2012) 2469–2477.
[10] X. He, G. Zhang, A.A. de la Cruz, et al., Environ. Sci. Technol. 48 (2014) 4495–4504.
[11] M.A. Oturan, J.-J. Aaron, Crit. Rev. Environ. Sci. Technol. 44 (2014) 2577–2641.
[12] N.F.F. Moreira, C. Narciso-da-Rocha, M.I. Polo-López, et al., Water Res. 135 (2018) 195–206.
[13] Y. Duan, L. Deng, Z. Shi, et al., Chem. Eng. J. 359 (2019) 1379–1390.
[14] S. Li, Z. Wang, X. Zhao, et al., Chem. Eng. J. 360 (2019) 600–611.
[15] C. Zhao, Z. Liao, W. Liu, et al., J. Hazard. Mater. 381 (2020) 120957.
[16] E. Brillas, C.A. Martínez-Huitle, Appl. Catal. B: Environ. 166–167 (2015) 603–643.
[17] S. Garcia-Segura, E. Brillas, J. Photochem, Photobiol. C: Photochem. Rev. 31 (2017) 1–35.
[18] J.D. García-Espinoza, P. Mijaylova-Nacheva, M. Avilés-Flores, Chemosphere 192 (2018) 142–151.
[19] K. Gurung, M.C. Ncibi, M. Shestakova, et al., Appl. Catal. B: Environ. 221 (2018) 329–338.
[20] W. Wang, Y. Lu, H. Luo, et al., Water Res. 139 (2018) 58–65.
[21] X. Cheng, H. Liu, Q. Chen, et al., J. Hazard. Mater. 254–255 (2013) 141–148.
[22] Q. Ma, H. Zhang, R. Guo, et al., Electrochim. Acta 283 (2018) 1154–1162.
[23] X. Cheng, H. Liu, Q. Chen, et al., Electrochim. Acta 103 (2013) 134–142.
[24] X. Cheng, Q. Cheng, X. Deng, et al., Chemosphere 144 (2016) 888–894.
[25] F. Zhang, S. Cheng, D. Pant, et al., Electrochem. commun. 11 (2009) 2177–2179.
[26] Y. Yuan, J. Wang, M. Yao, et al., J. Korean Inst. Electr. Electron. Mater. Eng. 47 (2018) 633–640.
[27] H. Wang, J.L. Wang, J. Hazard. Mater. 154 (2008) 44–50.
[28] X. Cheng, G. Pan, X. Yu, Chem. Eng. J. 279 (2015) 264–272.
[29] T. Xiao, Z. Tang, Y. Yang, et al., Appl. Catal. B: Environ. 220 (2018) 417–428.
[30] L. Jiang, X. Yuan, G. Zeng, et al., Appl. Catal. B: Environ. 227 (2018) 376–385.
[31] J. Zhang, Y. Hu, X. Jiang, et al., J. Hazard. Mater. 280 (2014) 713–722.
[32] X.Z. Li, F.B. Li, C.M. Fan, et al., Water Res. 36 (2002) 2215–2224.
[33] J. Ma, M. Sui, T. Zhang, et al., Water Res. 39 (2005) 779–786.
[34] S.Y. Zhou, Z.X. Zhong, Y.Q. Fan, et al., Chin. J. Chem. Eng. 17 (2009) 739–745.
[35] R.E. Palma-Goyes, F.L. Guzmán-Duque, G. Peñuela, et al., Chemosphere 81 (2010) 26–32.
[36] H. Jalife-Jacobo, R. Feria-Reyes, O. Serrano-Torres, et al., J. Hazard. Mater. 319 (2016) 78–83.
[37] X. Zhao, L. Guo, J. Qu, Chem. Eng. J. 239 (2014) 53–59.
[38] S. Periyasamy, M. Muthuchamy, J. Environ, Chem. Eng. 6 (2018) 7358–7367.
[39] I. Sirés, E. Brillas, M.A. Oturan, et al., Environ. Sci. Pollut. Res. 21 (2014) 8336–8367.
[40] M.N. Chong, B. Jin, J. Hazard. Mater. 199–200 (2012) 135–142.
[41] Y.F. Rao, L. Qu, H. Yang, et al., J. Hazard. Mater. 268 (2014) 23–32.
[42] M.M. Ahmed, S. Chiron, Water Res. 48 (2014) 229–236.